I.J. Information Technology and Computer Science, **2026, 1, 163-179**
Published Online on February 8, 2026 by MECS Press (http://www.mecs-press.org/)
DOI: 10.5815/ijitcs.2026.01.09

An Explainable AI Framework for Lung Cancer Detection Using Crested Porcupine Optimized Channel-Attention Inceptionresnet

Robert R.*
Department of Electronics and Communication Engineering, Kalasalingam Academy of Research and Education, Tamil Nadu, India
E-mail: robertrr4231@gmail.com
ORCID iD: https://orcid.org/0009-0000-9128-0543
*Corresponding author

Muneeswaran V.
Department of Electronics and Communication Engineering, Kalasalingam Academy of Research and Education, Tamil Nadu, India
E-mail: munees.klu@gmail.com
ORCID iD: https://orcid.org/0000-0001-8061-8529

Jose Saji Kumar
Principal, Grace Polytechnic College, Tamil Nadu, India
E-mail: josesrohit@gmail.com

Received: 28 July 2025; Revised: 24 September 2025; Accepted: 11 November 2025; Published: 08 February 2026

Abstract: Lung cancer is a main reason of death globally, and reducing death rates and enhancing treatment results depend heavily on quick identification. However, medical image diagnosis, including Computed Tomography (CT) scans, is difficult and demands a high level of experience. This research proposes a comprehensive and interpretable Computer-Aided Diagnosis (CAD) structure to identify lung cancer from medical images. The workflow initiates with an Adaptive Savitzky-Golay Filter, effectively enhancing image quality by smoothing while preserving critical structural edges. Hierarchical Adaptive Cluster Refinement (HACR) is then used for precise segmentation, adaptively identifying abnormal lung regions with high accuracy. For feature extraction, the proposed system utilizes the Deep Statistical Gray-Level Co-occurrence Matrix (DS-GLCM) approach, which captures deep spatial and statistical texture features essential for distinguishing cancerous tissue. At last stage, classification is performed using a novel Deep Learning (DL) model Crested Porcupine Optimized (CPO) Channel-Attention (CA) InceptionResNet. The CPO algorithm is exploited to tune the CA-InceptionResNet model's hyperparameters. To ensure transparency and reliability in clinical use, Explainable AI (XAI) technique- Local Interpretable Model-Agnostic Explanations (LIME) is used for visual interpretability, highlighting regions in CT images that contribute the most to model forecasts, thus boosting clinician trust and decision-making. The entire framework is implemented in Python, and experimental results on benchmark lung cancer imaging datasets demonstrate its superior performance in terms of performance metrics with an accuracy of 98.18% with sensitivity of 95.94 % and specificity of 99.10%. The combination of advanced DL and explainable AI makes the proposed framework a promising solution for lung cancer diagnosis.

Index Terms: Lung Cancer, Adaptive Savitzky-Golay Filter, HACR, DS-GLCM, Channel-Attention InceptionResNet, Crested Porcupine Optimization, AI (XAI) Technique.

1. Introduction

Globally, lung cancer is amid the cancers most commonly to be diagnosed in both women and men. Lung cancer has the greatest diagnosis rate amongst all cancers, which accounts for 11.6% of all cancer diagnoses; it also has the highest fatality rate of 18.4% over all cancer demises [1]. Few lung cancer patients receive a screening diagnosis; instead, the majority are identified after several symptoms appear [2]. However, the majority of lung cancer symptoms don't appear until the disease is considerably advanced, which makes therapy challenging. Nowadays, a number of criteria are examined to determine a patient's mortality risk, including age, smoking history, prior cancer history, family genealogy, and radiologic factors such tumor size and shape [3]. The diagnosis and treatment of patients and enhancement of survival greatly depend on quick and precise classification of lung cancer [4]. The first step in detecting lung cancer early is to observe for nodules. To support physicians in making medical diagnoses, the second phase involves classifying non-lung and lung cancer on CT scans of lung nodules. Physicians use a variety of methods like X-rays, MRIs, and biopsies are often invasive, costly, and time-consuming. Spotting small lesions early is especially difficult, making diagnosis challenging. While CT scans help, manually reviewing them is slow and lead to human error [5, 6].

Traditional techniques are often time consuming and costly, generating negative influence on comfort of patients. Henceforth, there is a need for cheaper, faster and less intrusive investigative methods [7]. Recent years, experienced momentous progression in artificial intelligence and DL architectures in treating cancers. Notably, DL models have proved improved performance in predicting anomalies and complex pattern by training a large dataset [8]. Numerous research has investigated a range of strategies, from existing machine learning algorithms to conventional statistical models [9-11]. In order to attain higher performance, this research integrates modern approaches to provide a novel approach to lung cancer prediction. Existing lung cancer detection approaches frequently have significant shortcomings, such as the loss of structural details during filtering, inefficient segmentation techniques, and inadequate feature representation owing to reliance on handcrafted or deep features alone. Overfitting and poor generalization result from the inflexible architectures and manual tuning used by many deep learning models. Furthermore, most approaches lack of interpretability erodes clinical trust. These gaps highlight the need for a more adaptive, explainable, and optimized framework, as proposed in this study.

The primary contributions consist of:

- Enhanced Image Preprocessing: Proposes an Adaptive Savitzky-Golay Filter for its ability to reduce noise while preserving critical lung edges.
- Precise Segmentation: Selected HACR for its adaptive clustering ability, which improves segmentation accuracy over static methods by dynamically updating centroids
- Robust Extraction of Features: DS-GLCM which enhances feature extraction by capturing deep statistical texture details, improving contrast and correlation
- Accurate Classification: Utilization of CPO-CA Inception ResNet architecture, combines attention and CPO algorithm to fine-tune the model, leading to high accuracy and robust classification
- Clinical Transparency: Incorporates LIME-XAI method to visualize model decision-making, showing which regions of the lung images most influence classification.

The rest of paper discuss about recent related works in lung cancer detection are reviewed, with an emphasis on advantages and disadvantages of current methods in Section 2. The proposed model, including its pre-processing, segmentation, feature extraction, classification, and explainability components, is detailed in Section 3. The CPO procedure is explained in Section 4. The incorporation of Explainable AI approaches is described in Section 5. Performance evaluation and experimental results are covered in Section 6. A comparison with baseline models is given in Section 7. Key findings and recommendations for additional research are included in Section 8, which concludes the paper.

2. Related Works

Many studies have been directed on the design of diagnosis systems for the screening of lung cancer. Several investigations were noteworthy for their identification and classification of lesions, their characterisation, and their classification as malignant. DL supported [12] research have recently produced extremely good and positive results in lung cancer screening. The proposed approach combines SVM classification with DL based extraction of features for the prediction of lung cancer in its primary stages [13]. Among its advantages are its high accuracy of 94%, reduced need for human feature engineering, and possible decrease in overfitting. The limitations include high processing requirements, dependence on huge datasets, and restricted comprehension of deep network characteristics. By dividing the task into several phases and utilizing, the modified U-Net and AlexNet-based technique seeks to provide extremely accurate lung cancer classification [14]. Although computational complexity, data needs, and interpretability are still continuing issues for practical application, its excellent performance on LUAN16 emphasizes its potential. For multi-scale feature extraction, two path Denoising First Convolutional Neural Network (DFD-Net) is proposed [15]. It is further improved by discriminant correlation estimation for a more accurate feature concatenation and a retraining technique to rectify label imbalance. Practical adoption is nevertheless restricted by the increasing processing load, implementation complexity, and requirement for huge, high-quality datasets. To detect lung cancer on LUNA16, a Deep Ensemble 2D CNN [16] integrates many CNNs with different layers, kernels, and pooling. It uses complimentary feature learning to attain higher accuracy (95%) than individual models. To avoid overfitting, it necessitates precise tuning, a large amount of training data, and increased processing needs. Using CT images, a CNN based on DenseNet-121, deep autoencoders, and MobileNet V3-Small identify and categorize lung cancer [17]. With fewer computational resources, an excellent precision of 98.6% and 95.8 Cohen's Kappa is made possible by quantization-aware training, early halting, and Adam optimization. With plans to integrate liquid neural networks and ensemble techniques for additional performance enhancements, the model supports real-time clinical diagnosis.

For nano-CT lung cancer diagnosis, in [18] a hybrid pipeline that combines Bag of Visual Words (BoVW) and Convolutional Recurrent Neural Network (CRNN). It greatly reduces segmentation time while achieving high performance with enhanced accuracy, exceptional precision, sensitivity, and specificity. Nevertheless, the method is computationally expensive and depends on specific segmentation algorithms that need to be further tested on a variety of clinical datasets. To improve the detection and localization of tiny tumors, Lung-RetinaNet based lung tumor detection system is discussed in [19], using multi-scale feature fusion in conjunction with a dilated module. By efficiently aggregating semantic data, it improves the accuracy of early detection and minimizes the need for human intervention. Its greater complexity, however, results in higher computing requirements and demands detailed clinical validation. The optimal models for various data splits, however, differ, necessitating an evaluation of the models' consistency across training samples. In order to ensure that a model focuses on pertinent aspects, Explainable AI (XAI) [20, 21] techniques particularly visual explanations demonstrate the important areas of images to support its predictions. This technique boosts the confidence and accuracy of diagnosis systems by contrasting appearances across different training samples. It also makes it possible to confirm that models trained on different data splits employ the same informative regions.

3. Proposed System Model

Fig. 1 depicts a structure for prediction of lung cancer utilizing CT images, integrating advanced approaches and explainability technique. The process starts with collection of CT images of lungs for diagnosing abnormalities and includes normal, benign and malignant cases. Pre-processing using an adaptive Savitzky-Golay filter is chosen over standard filters due to its ability to enhances the quality of CT image by removing noises with preservation of essential features. It significantly improves the contrast and clarity of edges that are crucial for segmentation. HACR segmentation model is preferred over conventional methods like U-Net in due to its data-light, adaptive behavior, particularly effective in handling variable tumour shapes in small datasets without requiring large-scale annotated data. The developed segmentation approach isolates the lung region and potential tumor areas effectively. It adaptively updates cluster centroids to accurately map lung regions and ensures non-overlapping, high-precision segmentation. Following segmentation, Deep Statistical GLCM based feature extraction is utilized to capture textural patterns and statistical dependencies within the lung tissues, serving as discriminative features for classification. These features are then fed into a Channel-Attention InceptionResNet model for Classification, which leverages both spatial attention and deep residual learning to accurately differentiate among normal and cancerous cases. This model enhances the network to adaptively weigh feature channels and effectively classify Lung CT images.

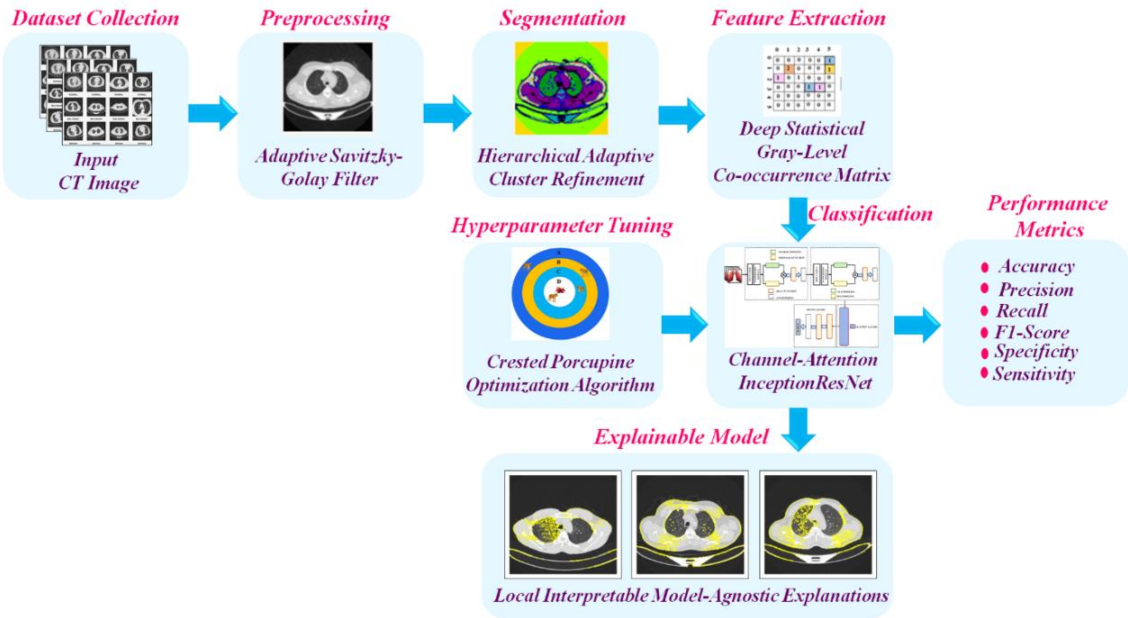

Fig.1. Developed block diagram

To optimize the performance of classification model, hyper parameter tuning including parameters layer configuration, leaning rate, attention depth is performed using CPO algorithm, inspired by defensive behavior of porcupines. This optimization balances exploration and exploitation, supporting model to converge to optimal structure for better performance. Finally, to assure transparency and reliability in the decisions of model, an explainable model component is integrated using LIME that provides visual and interpretable justifications of the classification results on

CT images, highlighting regions contributing to the prediction and aiding clinical decision-making. This increases transparency and trust that are essential for real world clinical deployment. The performance of model is assessed utilizing key Performance Metrics. These metrics ensure a well-rounded assessment, particularly critical in medical diagnosis, where false negatives have serious consequences.

3.1. Adaptive Savitzky-Golay Filter

To increase the Signal-to-Noise Ratio (SNR) while maintaining important image features including tumor borders, vascular architectures, and tissue textures, the adaptive savitzky golay filter is utilized to data taken from CT scan images of the lungs. The SG filter fits subsets of pixel intensity values with a low-order polynomial using a linear least squares approach, followed by convolution with resulting coefficients, in contrast to simple smoothing techniques that could obscure crucial diagnostic information.

The SG-filtered value Y_j at each point is calculated as follows given a sequence of n data points x_j, y_j, where x_j is the spatial index (e.g., pixel location along a row or column) and y_j represents corresponding CT intensity value.

$$Y_j = \sum_{i=(m-1)/2}^{(m-1)/2} C_i . y_{j+1} \; for \; \frac{m+1}{2} \leq j \leq n - \frac{m-1}{2} \tag{1}$$

The convolution coefficients in this case, C_i is determined using a chosen polynomial order (k) and frame size (f) or window length). The quality of noise reduction is assessed for each configuration by comparing the filtered output to a clean or synthetic reference image. The optimization criterion is the correlation coefficient (COR) between the reference and filtered is expressed as,

$$COR = \frac{\sum_{i=1}^{n}\left(X_i - \bar{X}\right)\left(\left(Y_i - \bar{Y}\right)\right)}{\sqrt{\sum_{i=1}^{n}(X_i - \bar{X})^2} . \sqrt{\sum_{i=1}^{n}(Y_i - \bar{Y})^2}} \tag{2}$$

Where $X = \{X_1, X_2, \ldots, X_n\}$ refers reference intensity profile, $Y = \{Y_1, Y_2, \ldots, X_n\}$ is the SG-filtered profile, and $\bar{X}, \bar{Y}$ are their respective mean values. An ideal filter setup is indicated by a COR value near 1.00, which successfully lowers noise while maintaining crucial anatomical features vital for the detection and analysis of lung cancer. The edge-preserving polynomial smoothing capacity of this method led to its selection over traditional filters. It successfully lowers noise while preserving distinct structural elements that are essential for precise segmentation and feature extraction, such as vascular edges and tumor boundaries. By maintaining these fundamental patterns, it helps HACR segmentation, increasing the final classification accuracy.

3.2. Hierarchical Adaptive Cluster Refinement-Segmentation Model

The hierarchical adaptive cluster refinement model aims to predict lung cancer by grouping CT images into clusters that represent similar tumor regions. The centroid is the average image for the cluster, formed by computing the average pixel values for matching pixels across all images within the cluster. This necessitates all images in the cluster to be of the same size or scaled to be uniform for accurate internal matching. A crucial requirement in this case is that the image has to be fall within a predetermined threshold distance from the cluster centroid. This image alone is used to establish a new cluster if no appropriate cluster discovered.

The average difference between the images color bands is used to calculate the distance between two image sizes. When comparing two images, $I \; and \; I'$, with dimensions of $r \times c$ pixels, the distance d between them is computed as follows,

$$d = \frac{1}{3rc} \sum_{x=0}^{c-1} \sum_{y=0}^{r-1} \sum_{z=RGB} \left| I_{x,y,z} - I'_{x,y,z} \right| \tag{3}$$

The centroid of a cluster is changed whenever a new image is added. The weighted average of the prior centroid and the new image is used to compute the new cluster representation in the event that a cluster with n images are expanded to include a new image I. This guarantees that the centroid approaches the updated image while staying inside the threshold's tolerance. The initial centroid is precisely the first image since the first cluster centroid is initialized with the first image. The centroid gradually moves to a point that is balanced across all of the photos in the cluster when more are added. The cluster representation of C' is expressed as,

$$C' = \frac{1}{n+1}\left(n.C + I\right) \tag{4}$$

The centroids constantly move as more images are analysed and added to the clusters, reflecting the evolving features of the images and improving the segmentation procedure. Crucially, this modification guarantees that no two clusters overlap, which is vital for the identification of lung cancer. To avoid confusion while distinguishing between healthy and malignant lung tissue, each image only be a part of one cluster at a time. When processing new CT images, HACR dynamically modifies cluster centroids and grouping boundaries according to spatial context and pixel intensity. Even in situations with low contrast, irregular tumor shapes, or overlapping tissues, this adaptive mechanism enables the model to hierarchically refine segmentation boundaries, resulting in more accurate isolation of abnormal lung regions. Furthermore, HACR makes sure that each region is uniquely assigned and avoids cluster overlap, both of which are essential for precise feature extraction and subsequent classification. After segmenting the image, which directed to DSGLCM approach for effective feature extraction as follows.

3.3. Deep Statistical Gray-Level Co-occurrence Matrix

By using deeper statistical descriptors across several spatial layers, DS-GLCM goes beyond traditional GLCM and detect minute texture variations that are frequently suggestive of malignant development in lung tissue. These characteristics, which include contrast, homogeneity, and entropy, are essential for spotting the uneven, varied patterns that are frequently present in cancerous areas. More accurate classification is supported by DS-GLCM's improved texture discrimination and robustness when compared to traditional GLCM. Analyzing the statistical correlations between pixel intensities at particular spatial locations within the image is the statistical method used in GLCM, also it extracts the features from the segmented image as demonstrated in Fig. 2.

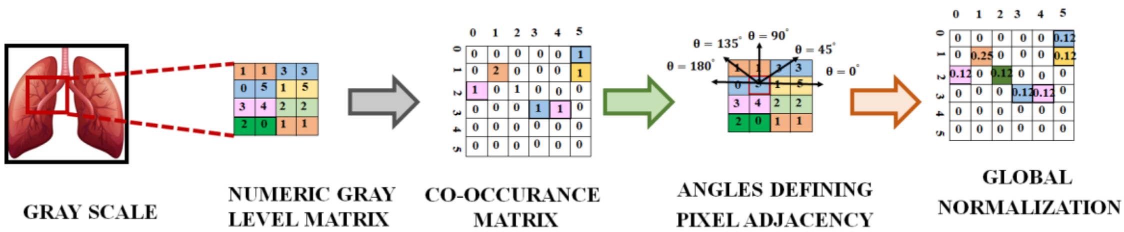

Fig.2. Model of GLCM based feature extraction

The mathematical representation of an image sample I with grayscale pixel values given by (x,y) and size $(M\,x\,N)$ is as follows.

$$G(I_{(x,y)}, I_{(x+d_x,y+d_y)})+1 \tag{5}$$

Following Equation (6) defines the normalized matrix $G_{norm(i,j)}$,

$$G_{norm(i,j)} = \frac{G_{(i,j)}}{T} \tag{6}$$

Where, $G_{norm(i,j)}$ signifies as a descriptive characteristics such as entropy, correlation, energy, contrast and homogeneity, T indicates number of valid pixel pairs, correspondingly. With the help of this model, the essential features from lung images are highly extracted, following this, the main classification is performed by channel-attention InceptionResNet as shown below.

3.4. Channel-Attention InceptionResNet

Joining the advantages of ResNet and the Inception model, the Inception-ResNet-V2 network is a potent DL architecture. For complicated image classification tasks of predicting lung cancer from CT scans, this architecture works incredibly well. Convolutions, batch normalization, activation functions, and pooling procedures are all mixed together in the model's layers, which process outlined in Fig. 3. The whole architecture is summed up as follows,

To extract initial features, I of size $H\times W\times C H\times W\times C$ (height H, width W, and channel's number (C) is processed through the first convolutional layers. Inception-ResNet blocks process the feature mappings from the preceding layer, convolutions in succession with varying kernel sizes,

$$Conv1(x) = ReLU(W_1 * x + b_1) \tag{7}$$

$$Conv3(x) = ReLU(W_3 * x + b_3) \tag{8}$$

Here, W denotes weight matrix, $*$ signifies the convolution layer and b stands for the bias term, respectively. In order to improve gradient flow during back propagation, additional connections are created between the convolution blocks' input and output,

$$Output(x) = ReLU(Conv1(x) + Conv3(x)) \tag{9}$$

Following the Inception-ResNet blocks, strided convolutions or pooling are used to reduce the spatial resolution, preserving key properties while lowering computational cost. The channel attention mechanism is integrated into Inception-ResNet-V2 architecture as outlined in Fig. 3, which enables the network to learn which feature channels such as various degrees of visual representations are more vital for differentiating among malignant and healthy lung tissue. The network concentrate on more discriminative features by adaptively weighting the channels, which increases the classification model's accuracy and resilience.

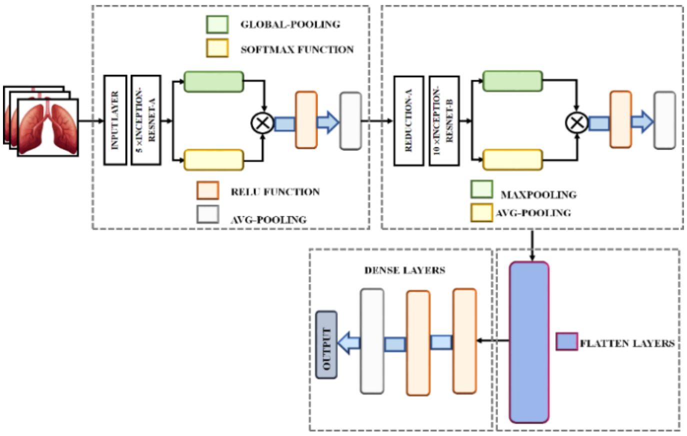

Fig.3. Structure Of Inception-ResNet-V2 with Channel Attention Model

Global Average Pooling (GAP) in the attention module allows the network to extract statistical data at the channel level. The following formula is used to determine each channel's statistical characteristic within an input feature map,

$$z_c = GAP(x_c) = 1/(H \times W) \sum_{i=1}^{H} \sum_{j=1}^{W} x_c(i, j) \tag{10}$$

In the equation above, z_c stands for a channel's statistical information, and x_c for the input features map. Furthermore, the input feature map's height and breadth are shown by H and W, respectively, and its spatial coordinates are shown by I and J. It has been noted that the squeeze-and-excitation (SE) block is equivalent to the channel attention module using GAP.

By combining two completely linked layers with ReLU and the Softmax activation function, the acquired data, denoted by Z, used to evaluate interconnections among channels.

$$s = \sigma(W_2 \delta(W_1 z) \tag{11}$$

The Sigmoid and ReLU nonlinear activation functions are denoted by σ and δ in the provided equation, respectively. Likewise, $W_1 \in R^{C \times C/r}$ and $W_2 \in R^{C/r \times C}$ are regarded as the dense layer weights. To increase the feature map count by C in W_2 and decrease the node count in W_1, use a reduction ratio r. The input feature map is then multiplied by scaling factors, which are found using the equation above.

$$\hat{x_c} = s_c \times x_c \tag{12}$$

In this case, where x_c indicates the $c-th$ channel of the rescaled feature map, and s_c stands for the $c-th$ channel of the scaling factors. The channel module is crucial for this study's regulation of global information in the ensemble technique.

Following the channel activation, undergo one or more fully connected layers and after being directed to flattened layer. After the dense layer, the last output layer calculates the classification probabilities,

$$\hat{y} = Softmax\left(W_f * x + b_f\right) \tag{13}$$

Where, weight matrix is W_f for the final layer, and bias is b_f. This output the probability distribution in the classes cancerous or non-cancerous. To get further improvement in the classification, the parameters from channel attention Inception-Resnet-V2 are fine-tuned by the integration of Crested Porcupine optimization algorithm. The channel-attention mechanism allows the model to shift its focus to discriminative feature maps, such as those showing aberrant texturing or tumor locations in lung CT images. Furthermore, the InceptionResNet architecture's critical hyperparameters are adjusted using CPO technique, which avoids local minima and increases convergence speed and classification accuracy. The model's combination of multi-scale feature learning, attention-driven focus, and CPO makes it extremely effective at capturing the minute and complex variations in lung cancer patterns.

4. Crested Porcupine Optimization Algorithm

The CPO algorithm is used for fine-tuning the hyperparameters of the Channel-Attention InceptionResNet model. Its multi-phase defense-inspired approach, which strikes a balance between exploration and exploitation guarantee improved convergence and classification performance. All around the world, with the exception of the Antarctic continent, the crested porcupine is a large rodent species. A wide range of environments, such as woodlands, rocky terrain, arid regions and sloping places, are home to it. An algorithm called the crested porcupine optimizer is developed in response to the crested defensive strategies of porcupine, which include four stages like visual, aural, olfactory and physical confrontation. These strategies are represented by four distinct search domains in the CPO architecture, each of which corresponds to a distinct porcupine defense zone. Zone A is the first stage of avoidance behavior, in which the perpetrator hides from possible dangers. Zone B is triggered, denoting the second line of defense, when this first strategy proves ineffective and predators continue to exist. Zone C is involved, signifying the third line of protection, if the predator is not deterred.When earlier tactics fail, the porcupiner turns to Zone D, its last line of defense, where it confronts the enemy directly in an attempt to defend itself and possibly neutralize it. Following steps illustrates the four stages and the flowchart view of this mentioned topology is displayed in Fig. 4.

Phase 1-Population Initialization: Start the search from a primary set of people (possible solutions) to initialize the population. The optimization issue in this study has three dimensions (3 parameters such as Convolution, channel attention, and flatten with dense layer). Each dimension's starting point is determined by initialization. This is accomplished using the following formula,

$$\vec{X}_i = \vec{L} + \vec{r} \times \left(\vec{U}_i - \vec{L}\right), I = 1,2,\ldots,N \tag{14}$$

Here, N signifies size of the population, X_i denotes number of candidate solutions and $\vec{U}$ and $\vec{L}$ are the upper and lower bounds. The following is a representation of the initial population:

$$X = \begin{bmatrix} X_1 \\ X_2 \\ \vdots \\ X_i \\ \vdots \\ X_N \end{bmatrix} = \begin{bmatrix} X_{1,1} & X_{1,2} & X_{1,3} \\ X_{2,1} & X_{2,3} & X_{2,3} \\ \vdots & \vdots & \vdots \\ X_{I,,1} & X_{i,2} & X_{i,3} \\ \vdots & \vdots & \vdots \\ X_{N,,1} & X_{N,2} & X_{N,3} \end{bmatrix} \tag{15}$$

Where, N indicates population size and $X_{i,j}$ is the jth location of the ith solution. Since there are just four model parameters to optimize, the dimension is taken as 4, which means that the highest value for j in $X_{i,j}$ is 3.

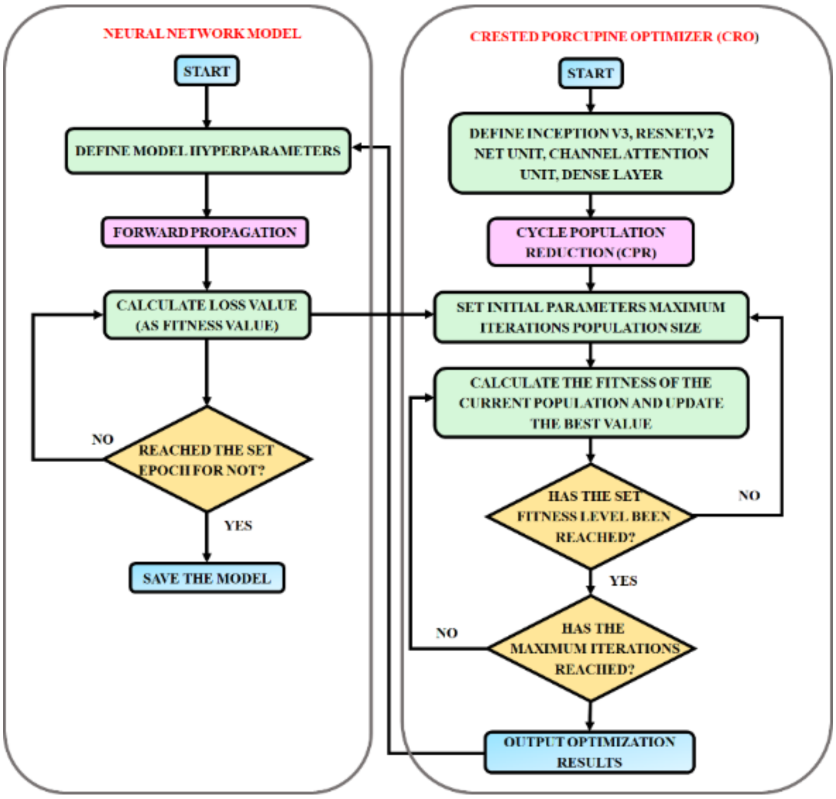

Fig.4. Flowchart representation of Inception-ResNet-V2 with channel attention optimized crested porcupine optimization

Phase 2: Method of Cycle Population Reduction (CPR) model: In order to speed up convergence, the CPR approach regularly reduces the population size though maintaining diversity. This tactic is comparable to Cape Porcupines' behavior, in which only those who feel a threat use their protection mechanisms. In order to speed up convergence, certain Cape porcupines are selected eliminated from the population in the optimization phase. They are then reintroduced to preserve diversity. This reduces the possibility of getting stuck in local minima. Equation (16) displays the cyclic population size lessening's mathematical model, where number of cycles is T, t is the function evaluation, highest evaluation function is T_{max} and N_{min} lowest number of newly formed population individuals.

$$N = N_{min} + \left(N' - N_{min}\right) \times \left(1 - \left(\frac{t \% \frac{T_{max}}{T}}{\frac{T_{max}}{T}}\right)\right) \tag{16}$$

Phase 3: Exploration Phase: The CP agitates its feathers in response to detecting a predator. The predator then has two choices: it moves closer to the CP, encouraging investigation of the region nearby to speed convergence, or it move away from the CP, allowing research of farther-off locations to find uncharted territory. Equation (16) is used to mathematically model this behavior.

$$\vec{x}_i^{i+1} = \vec{x}_i^t + \tau_1 \times \left|2 \times \tau_2 \times \right| \vec{x}_{CP}^t - \vec{y}_i^t \tag{17}$$

Where, $\vec{y}_i^t$ represents the predator's position at iteration t, τ_1 signifies a regularly distributed random value, τ stands for a random value in [0, 1], and $\vec{x}_{CP}^t$ represents the evaluation function $t's$ best solution.

The CP threatens the predator by making noises. The CP's groans get louder as the predator gets closer, which mathematically modelled using Equation (18),

$$\vec{x}_i^{i+1} = \left(1 - \vec{u}_1\right) \times \vec{x}_i^t + \vec{u}_1 \times \left(\vec{y} + \tau_3 \times \left(\vec{x}_{r1}^t - \vec{x}_{r2}^t\right)\right) \tag{18}$$

Here, t indicates a random number between [0,1], and r_1 and r_2 are 2 random integers among $[1, N]$.

Phase 4: Exploitation phase: Predators are discouraged from approaching when the CP produces an unpleasant odor that pervades its surroundings. Equation (15) models the behaviours.

$$\vec{x}_i^{t+1} = \left(1-\vec{R}_1\right)\times\vec{x}_i^t + \vec{R}_1\times\left(\vec{x}_{r1}^t + S_i^t\times\left(\vec{x}_{r2}^t - \vec{x}_{r3}^t\right) - \tau_3\times\vec{\delta}\times\gamma_t\times S_i^t\right) \tag{19}$$

Where, r_3 denotes random variable between $\left[1,N\right]$, γ_t specifies defensive factor, $\vec{x}_i^t$ specifies the *ith* person's position, and $\vec{\delta}$ governs the search direction. τ_3 Signifies random value among 0 and 1, and S_i^t denotes the diffusion factor for odor.

The CP uses physical force in response to an attacker who approaches to launch an attack. Equation (20) provides a mathematical representation of this contact, which is characterized as a one-dimensional non-elastic collision.

$$\vec{x}_i^{t+1} = \vec{x}_{CP}^t + \left(\alpha\left(1-\tau_4\right)+\tau_4\right)\times\left(\delta\times\vec{x}_{CP}^t - \vec{x}_i^t\right) - \tau_5\times\delta\times\gamma_t\times\vec{F}_i^t \tag{20}$$

Here, $\vec{F}_i^t$ denotes average force influencing the CP, τ_4 signifies random value among [1, 4], α indicates convergence rate factor, and $\vec{x}_{CP}^t$ stands for ideal solution obtained. The four CPO defense mechanisms mentioned above divided into two separate phases includes exploration and exploitation. A trade-off among the first and second defense mechanisms is carried out during the exploration phase. The third defense mechanism is used during the exploitation phase. Here is the condensed mathematical formula that we use to update the CP position,

$$\vec{x}_i^{i+1} = \begin{Bmatrix} \begin{cases} Apply\ equation\ (17) & \tau_6 < \tau_7 \\ Apply\ equation\ (18), & Else \end{cases} . \tau_8 < \tau_9\ _{(Exploration)} \\ ine \begin{cases} Apply\ equation\ (19) & \tau_{10} < T_{f.\tau_9 \le \tau_8 (Exploitation)} \\ Apply\ equation\ (20), & Else \end{cases} \end{Bmatrix} \tag{21}$$

Where, $\tau_6, \tau_7, \tau_8, \tau_9$ and τ_{10} are produced within 0 to 1 that consequently normalized to derive the optimal outcome $\vec{x}_i^{t+1}$. The population to be optimized in this study consist of the number of Inception-ResNet-V2 units, channel attention rate, flatten and dense rate, all of which treated as optimization factors. The fitness function for iterative optimization will be the loss function of neural network, which provide effectual better performance analysis and accurate identification.

5. Explainable AI Technique

LIME is designed to offer transparent and understandable clarifications for the forecasts prepared by complex, black-box models. In prediction of lung cancer, LIME generates perturbations by selectively activating or deactivating specific superpixels in CT scans. This approach helps to clarify the decision-making process, making it easier for healthcare professionals to interpret the importance of particular superpixels in determining the presence of lung cancer. Through this method, LIME highlights which regions of the image contribute most to the model's prediction, offering valuable insights into the diagnostic reasoning. LIME enhances the interpretability of models and fosters transparency, thereby increasing confidence in DL systems. By clarifying how different input characteristics, such as tumor size or texture, influence model predictions, LIME allows healthcare professionals to better understand the decision-making process. The first step in applying LIME to a medical image, such as a CT scan, is to break it down into superpixels groups of connected pixels that share similar color and spatial proximity. This decomposition improves the quality of the explanations provided, enabling more precise insights into how specific regions of the image, like tumors, contribute to the prediction of lung cancer. In turn, this leads to better-informed clinical decision-making and supports more trustworthy applications of AI in healthcare.

6. Result and Discussions

The developed explainable AI for detection of lung cancer using Crested Porcupine Optimized Channel-Attention is implemented in Python software, which is analyzed in this section. The IQ-OTH/NCCD lung cancer dataset is collected over three months in the fall of 2019 from the Iraq Oncology Teaching Hospital and the National Center for Cancer Diseases. It contains 1190 slices from 110 CT scans, of which 55 are normal, 40 are cancer and 15 are benign. The training stage comprises 833 images while testing contains 357 images.

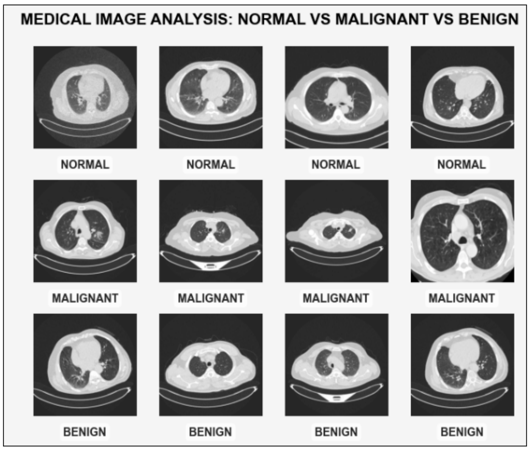

Fig.5. Input image

Fig. 5 represents an input image utilizing CT scans that is classified into normal, malignant and benign cases. The normal lung images are characterised by no abnormal tissues or visible lesions, indicating healthy lung tissue. Then, the malignant type differentiated by abnormal shape, clear masses or significantly altered textures indicating the aggressive growth of cancer tissues. Subsequently, the benign type is appeared as smoother and more regular, lacking the intense contrasts in malignancy. Efficient prediction of these images via CAD tools aids clinicians in the accurate forecast and distinction of lung cancer types, enabling appropriate clinical interventions.

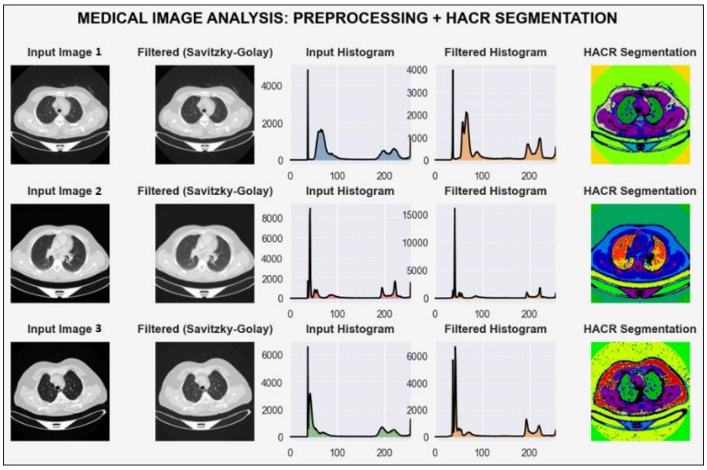

Fig.6. Pre-processed and segmented image

The pre-processed and segmented image in prediction of lung cancer is displayed in Fig. 6. It considers 3 distinct lung CT images, which are pre-processed utilizing Adaptive Savitzky-Golay filter that efficiently reduces noise and improving quality though preserving significant details for precise prediction of lung disease. Conversely, histograms before and after filtering denote variations in distributions of pixel intensity, representing enhanced image contrast and quality. Consequently, segmentation is performed utilizing HACR efficiently dividing each filtered image into different regions, distinguishing normal tissues from abnormal areas with high precision. The segmented images indicated with separate colors, enable exact characterisation of lung lesions, helping doctors in precisely detecting lung cancer.

Table 1. Feature extraction with DS-GLCM

Input Images/Features	1	2	3
Contrast	140.10	164.99	187.67
Dissimilarity	5.34	5.19	5.76
Homogeneity	0.38	0.55	0.45
Energy	0.07	0.22	0.12
Correlation	0.99	0.99	0.98
ASM	0.00	0.05	0.01

The features of DS-GLCM with distinct input images are represented in Table 1. An input image 3 has the highest contrast of 187.67 and dissimilarity of 5.76, while the input image 2 has the highest homogeneity of 0.55 and energy of

0.22. Subsequently, the correlation is same for both input image 1 and 2 whereas, the input image 2 has 0.05 Angular Second Moment (ASM) value, allows the extraction of valuable data for further classification.

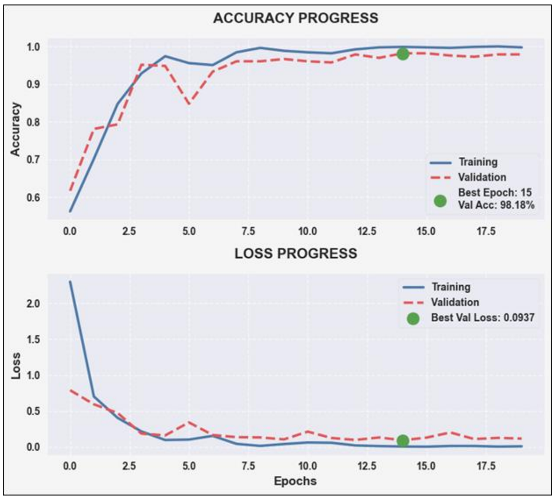

Fig.7. Training and validation results

Fig. 7 depicts the training and testing results for prediction of lung cancer. The accuracy increases, stabilizing close to the better performance at epoch 15, while the validation accuracy has the value of 98.18%. Meanwhile, loss graph, indicating the reduction of error rates for both training and validation datasets. The training loss initially declined and progressively steadies, indicating effective learning without overfitting. Here, the validation loss reduces constantly, reaching a reduced value of 0.0937 at epoch 15. It reveals the proposed approach attains better accuracy and minimal loss, denoting robust performance and reliability in the recognition of lung cancer.

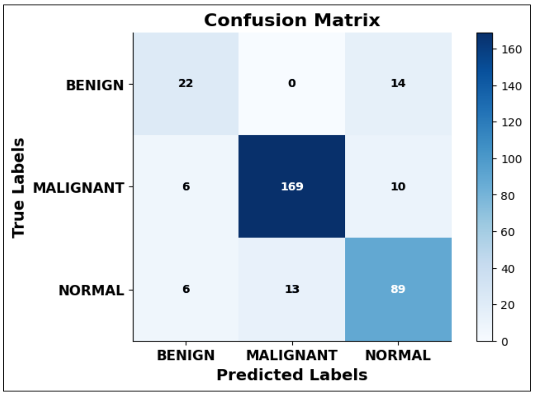

Fig.8. Confusion matrix

Fig. 8 reveals the confusion matrix denoting the classification performance of a detection of lung cancer, distinguishing among 3 cases. It properly depicts the precise and improper detections for each class. The malignant class has the maximum accuracy with 169 properly detected instances, denoting better performance in finding lung cancer. Also, the benign class has 22 proper detections and 14 as misclassifications that are improperly labeled as normal. Likewise, normal cases are detected with better accuracy, because 89 cases correctly predicted and also, normal classes misclassified as benign or malignant. The occurrence of some misclassifications denotes the need for further enhancement, highlighting the necessity for improved training data to diminish false negatives and positives, enhancing the reliability of lung cancer prediction.

The Receiver Operating Characteristic (ROC) curve for a lung cancer prediction is indicated in Fig.9. The Area Under Curve (AUC) values denotes the reliable performance with the malignant type attaining maximum AUC value of 0.969144, denoting the excellent accuracy in properly detecting cancer cases. Then, the benign class has the AUC of 0.956011, representing the accurate differentiation of benign lesions. Similarly, the normal class denotes better performance with an AUC of 0.952991, revealing the reliability in properly classifying normal cases.

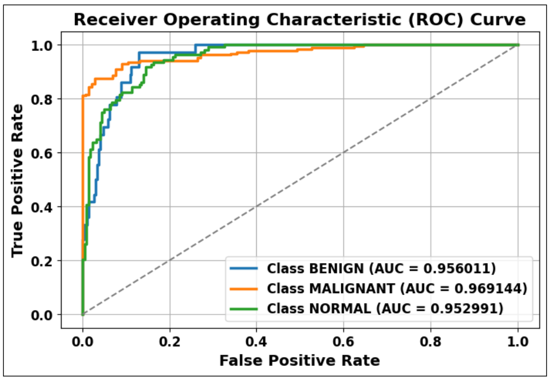

Fig.9. ROC curve

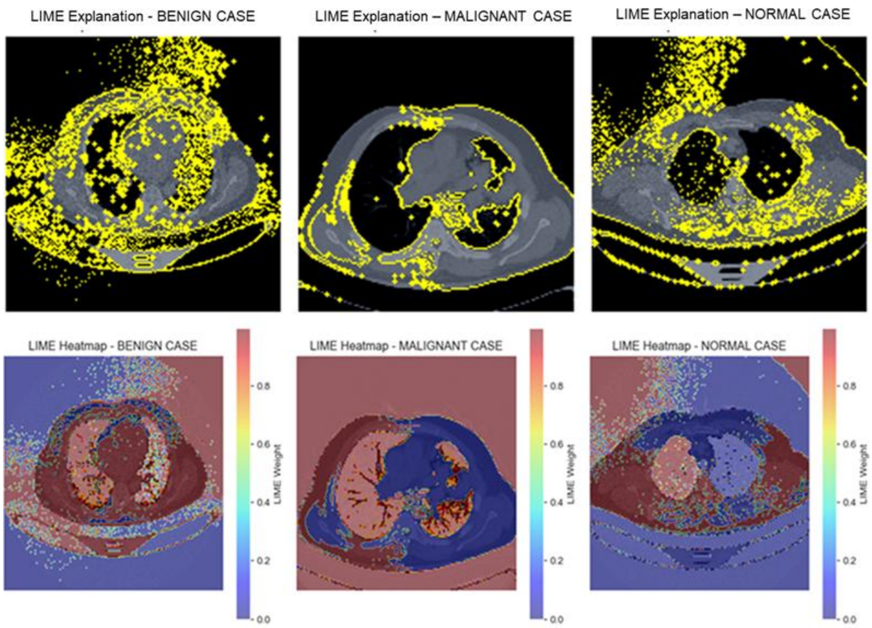

Fig.10. Explainable AI

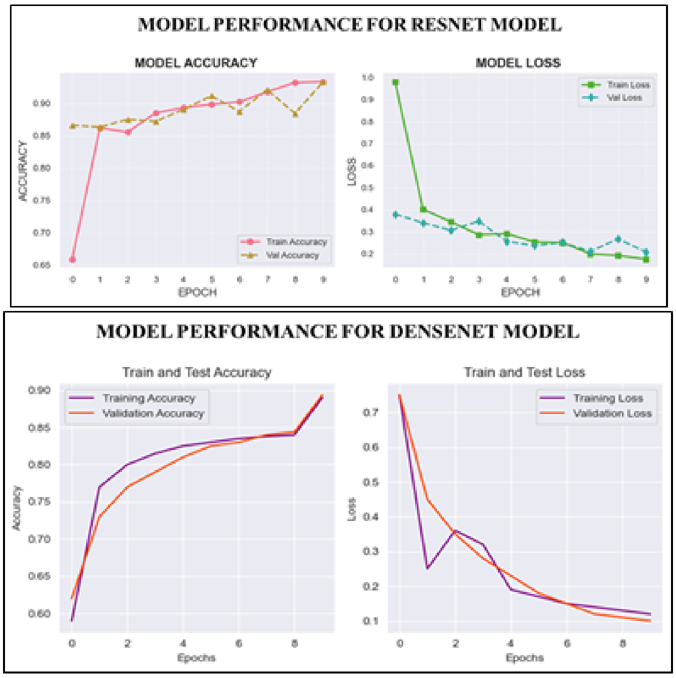

Fig.11. Training and validation results

Fig. 10 illustrates the series of CT scans of lungs, covered with visual representation of produced by an Explainable AI and heat map in prediction of lung cancer. The yellow regions denote areas of image that contributed to the prediction of model, indicating where the DL model focused its analysis during analysis. These visualization approach attained via saliency maps or class activation mappings (CAM) that aid clinicians interpret the decision-making process of AI by relating it with visible abnormalities. In this case, the highlighted regions related to potential tumor affected areas or other abnormal growths with in the lung lobes. By spotting critical zones, the XAI not only improves the transparency and reliability of AI driven diagnosis but acts as a proper tool in aiding clinical validation and diminishing diagnostic errors. This incorporation of interpretability into automated diagnostic systems is vital for clinical deployment, especially in sensitive applications like lung cancer detection. The bottom rows have a LIME heat maps where warmer colours highlight areas contributing most to the prediction of lung cancer.

Fig. 11 depicts the Training and Validation Results for ResNet and Dense Net model. The ResNet has a steady increase in accuracy with better convergence over 10 epochs. Then, the Dense Net has a high accuracy with in fewer epochs and sustain a low loss value.

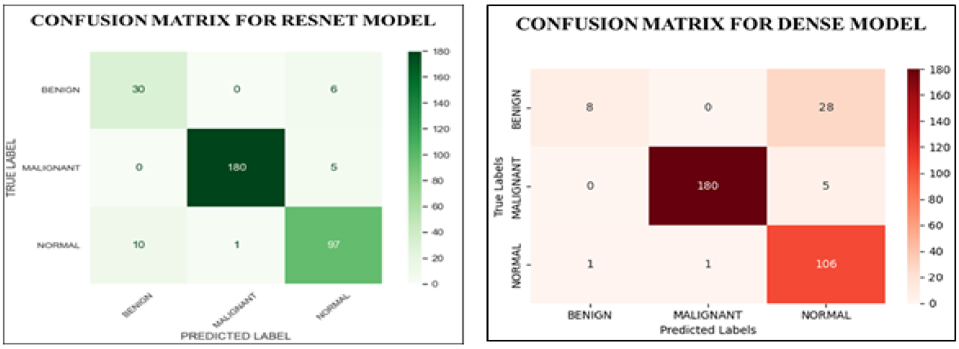

Fig.12. Confusion matrix

The Confusion matrix for ResNet and Dense Net model is shown in Fig. 12. The ResNet has high accuracy with minimal misclassifications over 3 classes. Then, the Dense Net attains better malignant classification but misclassifies the 28 benign cases. Dense Net performs well but has a maximum false negative rate in benign cases.

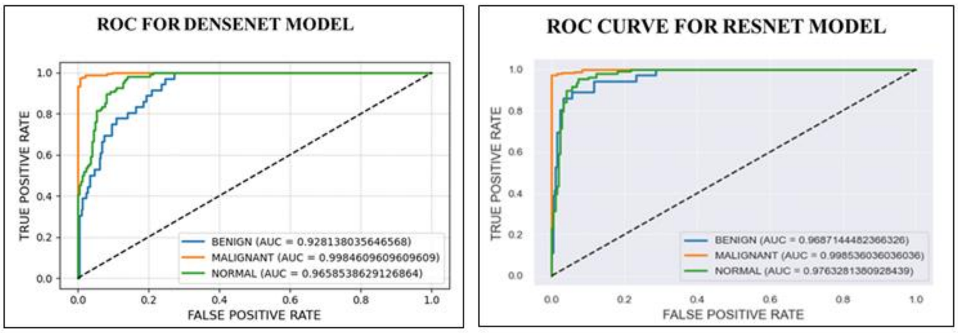

Fig.13. ROC curve

The ROC Curve for ResNet and Dense Net model is displayed in Fig. 13. The ResNet has the high ROC of 0.9965 in malignant case. Then, the Dense Net model has a high ROC of 0.9984 in the malignant case. It reveals the high reliability of earlier lung cancer prediction.

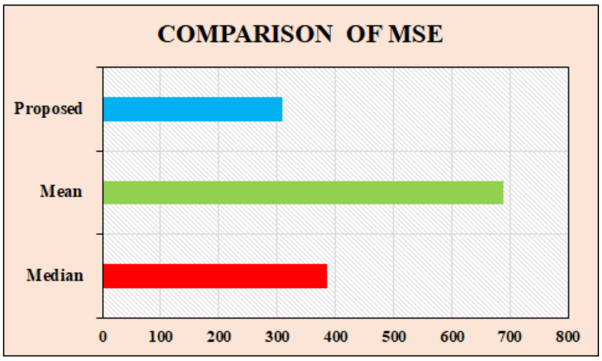

Fig.14. Comparison of MSE

The comparison of Mean Squared Error (MSE) for Mean [22], Median [23] and developed preprocessing approach is shown in Fig.14. The lowest MSE is attained by the Adaptive Savitzky-Golay Filter, which efficiently enhances the reliability of classification model.

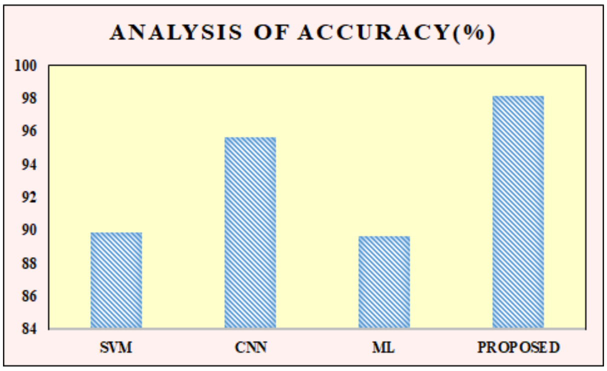

Fig.15. Analysis of accuracy

The analysis of accuracy for SVM [24], CNN [25], ML [26] and developed approach is represented in Fig. 15. The developed approach attains the highest accuracy of 98.18% than other approaches, indicating the performance is enhanced in predicting the lung cancer.

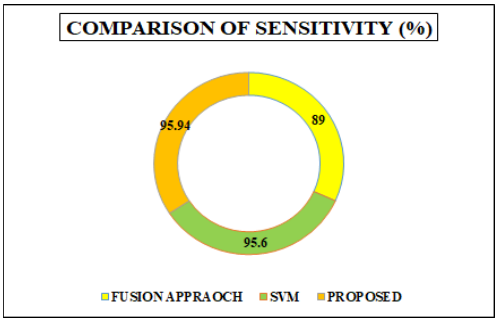

Fig.16. Analysis of sensitivity

Fig. 16 depicts an analysis of sensitivity for fusion approach [27], SVM [28] and developed approach, which has the maximum sensitivity of 95.94 % compared to other approaches, representing the lung cancer is detected in an early stage.

Table 2. Comparative analysis of precision

APPROACHES	PRECISION (%)
SVM [24]	95.6
CNN [29]	96.89
Proposed	98.25

The comparative analysis of precision for SVM, CNN and developed approach is displayed in Table 2. The highest precision value of 98.25% denoting the reliability and diagnostic accuracy is enhanced.

The analysis with existing approaches in terms of performance metrics is revealed in Table 3. Here, the proposed approach has the highest performance metrics value than ResNet and Dense Net approaches. The proposed system aids radiologists by automatically detecting the cancer regions in CT scans. The high sensitivity value assures the initial stage tumours are quickly predicted aiding the appropriate intervention. For real world application, the developed research is need to be tested on diverse datasets from various hospitals to assure robustness in varying imaging conditions. Its computational cost comprising processing time and memory usage needs assessment to confirm its suitability for deployment in hospital. Incorporation into radiologist's work flow needs a user friendly interface that highlights key diagnostic regions and aligns with existing systems.

Table 3. Analysis with existing approaches

Proposed Approach			
Classes	Precision	Recall	F1-score
Normal	0.9474	1.0000	0.9730
Malignant	1.0000	0.9892	0.9946
Benign	1.0000	0.8889	0.9412
ResNet			
Normal	0.8981	0.8981	0.8981
Malignant	0.9945	0.9730	0.9836
Benign	0.7500	0.8333	0.7895
Dense Net			
Normal	0.7626	0.9815	0.8583
Malignant	0.9945	0.9730	0.9836
Benign	0.8889	0.2222	0.3556

7. Conclusions

The present research focused on a novel CPO Channel-Attention InceptionResNet approach for lung cancer prediction by integrating advanced segmentation and classification techniques. Adaptive Savitzky-Golay filter effectively enhances image quality by smoothing while preserving critical structural edges. HACR adaptively group image regions based on spatial and intensity similarities and refines clusters to ensure non-overlapping, high-precision segmentation of abnormal lung tissue, thereby improving the accuracy of downstream processing Moreover, DS-GLCM enhances traditional texture analysis by incorporating deeper statistical measures across multiple spatial levels, allowing more discriminative feature extraction between malignant and benign tissues. The CPO-channel-attention InceptionResNet diagnostically provide relevant features and enhance classification performance. The incorporation of CPO further enhanced feature selection, focusing the model on diagnostically significant regions. LIME based XAI approach is incorporated to provide model's visual interpretability decisions and emphasizing regions contributing most to the diagnosis. This enables radiologists to interpret and validate predictions confidently. The entire framework is implemented in Python results shows a benchmark lung cancer imaging datasets demonstrate its superior performance in terms of performance metrics with an accuracy of 98.18%% than SVM, CNN and ML approaches. This topology holds great potential for enhancing early lung cancer identification in clinical practice.

References

[1] S. Oh, J. Im, S. R. Kang I. J. Oh, M. S. Kim, "PET-based deep-learning model for predicting prognosis of patients with non-small cell lung cancer," *IEEE Access,* no.9, pp.138753-138761, 2021.

[2] S. Matte, S. Mengal, T. Jadhav, P. Jadhav, P. Khawale, A. Khachane, D. G. Takale, "Prostate cancer detection using deep learning and traditional techniques," *IEEE Accessm,* no. 9, pp. 27085-27100, 2021.

[3] Y. Chen, Y. Wang, F. Hu, L. Feng, T. Zhou, C. Zheng, "LDNNET: towards robust classification of lung nodule and cancer using lung dense neural network," *IEEE Access,* no. 9, pp. 50301-50320, 2021.

[4] R. Robert, V. Muneeswaran, "Current Technology Development in Cancer Detection using Artificial Intelligence: Methodical Exploration and Interpretation," *In 2025 International Conference on Intelligent Systems and Computational Networks (ICISCN),* pp. 1-7. 2025.

[5] M. Malafaia, F. Silva, I. Neves, T. Pereira, H. P. Oliveira, "Robustness analysis of deep learning-based lung cancer classification using explainable methods," *IEEE access,* no.10, pp. 112731-112741, 2022.

[6] X. Fu, L. Bi, A. Kumar, M. Fulham, J. Kim, "An attention-enhanced cross-task network to analyse lung nodule attributes in CT images," *Pattern Recognition*, vol.126, pp. 108576, 2022.

[7] D. Riquelme M. A. Akhloufi, "Deep learning for lung cancer nodules detection and classification in CT scans," *AI*, vol. 1, no. 1, pp. 28–67, Jan. 2020.

[8] B. Ozdemir, E. Aslan, I. Pacal, "Attention Enhanced InceptionNeXt Based Hybrid Deep Learning Model for Lung Cancer Detection," *IEEE Access*, 2025.

[9] E. Dritsas, M. Trigka, "Lung cancer risk prediction with machine learning models," *Big Data and Cognitive Computing,* vol. 6, no. 4, pp. 139, 2022.

[10] V. Rajasekar M. P. V aishnnave, S. Premkumar, V. Sarveshwaran, V. Rangaraaj, "Lung cancer disease prediction with CT scan and histopathological images feature analysis using deep learning techniques," *Results in Engineering,* no.18, pp. 101111, 2023.

[11] X. Guan, Y. Du, R. Ma, N. Teng, S. Ou, H. Zhao, X. Li, "Construction of the XGBoost model for early lung cancer prediction based on metabolic indices," *BMC medical informatics and decision making*, vol. 23, no. 1, pp. 107, 2023.

[12] G. Kasinathan, S. Jayakumar, "Cloud-Based Lung Tumor Detection and Stage Classification Using Deep Learning Techniques," *Biomed research international*, vol. 2022, no. 1, pp. 4185835, 2022.

[13] I. Shafi, S. Din, A. Khan, I. D. L. T. Díez, R. D. J. P. Casanova, K. T. Pifarre, I. Ashraf, "An effective method for lung cancer diagnosis from CT scan using deep learning-based support vector network," *Cancers,* vol.14, no. 21, pp. 5457, 2022.

[14] I. Naseer, S. Akram, T. Masood, M. Rashid, A. Jaffar, "Lung cancer classification using modified u-net based lobe segmentation and nodule detection," *IEEE Access*, no. 11, pp. 60279-60291, 2023.
[15] W. J. Sori, J. Feng, A. W. Godana, S. Liu, D. J. Gelmecha, "DFD-Net: lung cancer detection from denoised CT scan image using deep learning," Frontiers of Computer Science, no. 15, pp. 1-13, 2021.
[16] A. A. Shah, H. A. M. Malik, A. Muhammad, A. Alourani, Z. A. Butt, "Deep learning ensemble 2D CNN approach towards the detection of lung cancer," *Scientific reports*, vol. 13, no. 1, pp. 2987, 2023.
[17] A. R. Wahab Sait, "Lung cancer detection model using deep learning technique," *Applied Sciences*, vol.13, no. 22, pp. 12510, 2023.
[18] A. SU, F. R. PP, A. Abraham, D. Stephen, "Deep learning-based BoVW–CRNN model for lung tumor detection in nano-segmented CT images," *Electronics*, vol. 12, no. 1, pp. 14, 2022.
[19] R. Mahum, A. S. Al-Salman, "Lung-RetinaNet: Lung cancer detection using a RetinaNet with multi-scale feature fusion and context module," *IEEE Access*, no. 11, pp. 53850-53861, 2023.
[20] M. K. Islam, M. M. Rahman, M. S. Ali, S. M. Mahim, M. S. Miah, "Enhancing lung abnormalities detection and classification using a Deep Convolutional Neural Network and GRU with explainable AI: A promising approach for accurate diagnosis," *Machine Learning with Applications*, no. 14, pp. 100492, 2023.
[21] M. Z. Hasan, S. Montaha, I. U. Khan, M. M. Hassan, A. Al Mahmud, A. R. H. Rafid, S. Azam, A. Karim, S.Prountzos, "Fast and efficient lung abnormality identification with explainable AI: A comprehensive framework for chest CT scan and X-ray images," IEEE Access, no. 12, pp. 31117-31135, 2024.
[22] C. Anam, K. Adi, H. Sutanto, Z. Arifin, W. S. Budi, T. Fujibuchi, G. Dougherty, "Noise reduction in CT images using a selective mean filter," *Journal of biomedical physics & engineering*, vol. 10, no. 5, pp. 623, 2020.
[23] S. A. Ştefănigă, "Fine-Tuned Medical Images Denoising using Median Filtering," *Applied Medical Informatics,* no. 43, pp. 27-27, 2021.
[24] H. F. Kareem, M. S. AL-Husieny, F. Y. Mohsen, E.A. Khalil, Z. S.Hassan, "Evaluation of SVM performance in the detection of lung cancer in marked CT scan dataset," *Indonesian Journal of Electrical Engineering and Computer Science*, vol. 21, no. 3, pp. 1731, 2021.
[25] A. Asuntha, A. Srinivasan, "Deep learning for lung Cancer detection and classification. Multimedia Tools and Applications," pp 1-32, 2020.
[26] S. Shanthi, N Rajkumar, "Lung Cancer Prediction Using Stochastic Diffusion Search (SDS) Based Feature Selection and Machine Learning Methods," *Neural Processing Letters*, vol.53, no. 4, 2020
[27] I. Nazir, I. U. Haq, M. M. Khan, M. B. Qureshi, H. Ullah, S. Butt, "Efficient pre-processing and segmentation for lung cancer detection using fused CT images," *Electronics*, vol. 11, no. 1, pp. 34, 2021.
[28] D. M. Abdullah, A. M. Abdulazeez, A. B. Sallow, "Lung cancer prediction and classification based on correlation selection method using machine learning techniques," *Qubahan Academic Journal*, vol. 1, no. 2, pp. 141-149, 2021.
[29] A. A. Abd Al-Ameer, G. A. Hussien, H. A. Al Ameri, "Lung cancer detection using image processing and deep learning," *Indones. J. Electr. Eng. Comput*. Sci., vol. 28, no. 2, pp. 987-993, 2022).

Authors' Profiles

Mr. R. Robert received his B.E. degree in Electronics and Communication Engineering from Francis Xavier Engineering College in 2014, under Anna University, and his M.E. degree in Applied Electronics from SCAD College of Engineering and Technology in 2017, affiliated with Anna University, Chennai. He is currently pursuing his Ph.D. in the field of Medical Image Processing at Kalasalingam Academy of Research and Education (KARE). In addition, he is enrolled in a Post Graduate Certification Program in Artificial Intelligence and Data Science at IIIT Kottayam, offered in hybrid mode. He serves as an Assistant Professor in the Department of Electronics and Communication Engineering at Stella Mary's College of Engineering, Nagercoil, and also holds the position of Vice President at Delta Box Technologies, where he actively contributes to innovation and industry collaboration. Mr. Robert has published more than 10 research papers in reputed international journals and has presented five papers at national and international conferences. He has also organized several sponsored seminars, workshops, faculty development programmes, and international conferences. His research interests include Medical Image Processing, Internet of Things (IoT), and Machine Learning.

Dr. V. Muneeswaran holds a Ph.D degree in Electronics and Communication Engineering and have vast research experience in discipline of Swarm Intelligence, Image/Signal Processing. He serves as a Guest editor for Applied Soft Computing, a peer reviewed journal published by Elsevier. As an author has published several articles in reputed journals Journal of Supercomputing, IEEE Access, Cognitive Systems Research and also several works as Book Chapters in Lecture notes in Computer Science, Advances in Intelligent Systems and Computing, Lecture Notes in Electrical Engineering and Smart Innovation, Systems and Technologies published by Springer. Majority of the articles published was based on the application of swarm intelligence for engineering applications viz., Medical Image Segmentation, optimization of Neural Networks etc., On his credit, there are several awards including Publons Peer Review Awards 2018 for placing in the top 1% of reviewers in Computer Science. At present he is working on projects related to Brain tumor segmentation using swarm intelligence techniques and Key areas in Medical Image Segmentation.

Mr. F. Jose Saji Kumar received his B.E. degree in Electronics and Communication Engineering from Government College of Engineering (formerly called as IRTT), Erode in 2000, under Bharathiar University, Coimbatore and his M.E. degree in Applied Electronics from Anna University, Tirunelveli in 2012, affiliated with Anna University, Chennai. He is currently pursuing his Ph.D. in the field of Medical Image Processing at Kalasalingam Academy of Research and Education (KARE). He serves as a Principal, Grace Polytechnic College, Thoothukudi. Mr. F. Jose Saji Kumar has published more than 10 research papers in reputed international journals and has presented five papers at national and international conferences. He has also organized several sponsored seminars, workshops, faculty development programmes, and international conferences. His research interests include Medical Image Processing, Internet of Things (IoT), and Machine Learning.

How to cite this paper: Robert R., Muneeswaran V., Jose Saji Kumar, "An Explainable AI Framework for Lung Cancer Detection Using Crested Porcupine Optimized Channel-Attention Inceptionresnet", International Journal of Information Technology and Computer Science(IJITCS), Vol.18, No.1, pp.163-179, 2026. DOI:10.5815/ijitcs.2026.01.09